Transforming Decentralized Wastewater Treatment with Fibrous Super-Bridging Agents and a Compact Reactor

Mathieu Verhille[1], Emilia Tognetty[1], Manel Mebarki[1], Lovenie Victor[1], Masashi Kaneda[2], Owen Armstrong[2], Nathalie Tufenkji[2] and Mathieu Lapointe[1]*
[1] University of Québec – École de technologie supérieure, Montréal, Québec, H3C 1K3, Canada
[2] Department of Chemical Engineering, McGill University, Montreal, QC, H3A 0C5, Canada
* Corresponding author

Abstract

Ageing sewer networks and increasingly variable wastewater characteristics motivate the development of compact, versatile, and high-rate treatment strategies capable of operating with short residence times and reduced operational costs. Here, we present a decentralized fiber-assisted coagulation–flocculation–floc separation "3-in-1" approach that integrates rapid floc separation via settling and coarse screening to enable decentralized pretreatment. Floc size distribution analyses demonstrated that fibers markedly increased floc size compared with conventional treatment, enabling rapid clarification to ≤ 25 NTU and residual TSS as low as ~1 mg-TSS·L^{-1}. Screening through a 200 to 2000-µm mesh provides an additional safeguard when gravity separation is limited, while simultaneously facilitating in-line solids capture and sludge dewatering suitable for compact system designs. Modification of fibers with targeted surface chemistries further expands treatment capability by enabling nutrient-specific capture; namely, iron-grafted fibers reduced residual total phosphorus concentrations to approximately 1 mg-TP·L^{-1}. Pilot tests in a 178-L integrated module achieved ≤ 25 NTU on an extremely turbid wastewater stream (up to 4500 NTU; > 99 % removal), demonstrating process scalability and applicability. This study introduces a regenerable and tunable fiber-enabled platform for high-rate clarification using a simple separation approach, offering a practical pathway toward resilient, decentralized wastewater management while reducing reliance on conventional centralized treatment plants – which are already under increasing pressure from rising flows and treatment demands.

Keywords: Coagulation-flocculation; High-rate aggregation; DEWATS; Water pollution; Sustainable water management

Main

Centralized collection and treatment systems remain the standard for wastewater management, serving nearly 80% of the population across half of OECD countries. These systems remain essential, but the local treatment of specific wastewater streams may reduce the pollutant loads transferred to sewer networks and downstream treatment plants[1–5]. This approach is particularly relevant for industrial effluents, which can differ markedly in suspended solids, colloidal composition, organic matter and the presence of nutrients and micropollutants[6–9]. Although industrial discharges may represent only a limited fraction of the total influent flow, their concentration can disproportionately increase treatment requirements and disrupt process stability at wastewater treatment plants[10–14]. Such concentrated or intermittent inputs can disrupt biological nutrient removal[15], require flow equalization to attenuate variations in flow and organic loading[16], increase aeration demand[10] or necessitate additional chemical conditioning[17] to maintain stable effluent quality.

Coagulation–flocculation has increasingly been incorporated into compact treatment configurations by coupling chemical aggregation with direct filtration, microsieving or ballasted settling[18–23]. Nevertheless, producing flocs that are simultaneously large, mechanically robust and readily separable remains a challenge in heterogeneous wastewaters[24–27]. Notable demonstrations include the CFFA process, which couples alum and anionic-polymer flocculation with micromesh filtration for rapid on-site stormwater treatment[18]. Ballasted flocculation instead incorporates microsand into the aggregates to accelerate settling [19]. Although promising, these approaches require micromesh filtration or controlled ballast addition and have been validated on a single or simplified water matrix. Few studies have jointly assessed whether coagulant demand can be reduced while maintaining rapid settling, coarse-screen retention and effective post-separation solids handling across chemically distinct real wastewaters.

Recently, fiber-assisted coagulation–flocculation has emerged as a floc-structuring approach in which fibrous materials[28], acting as super-bridging agents, promote the formation of larger, mechanically robust flocs, thereby enabling faster separations[28,29]. Cellulose fibers offer a tunable surface chemistry, enabling the grafting of specific capture sites for contaminant removal[30–32]. Such functionalization could extend fiber-assisted primary treatment to selected source-specific contaminants[33]. However, most demonstrations have focused on synthetic waters or specific wastewater matrices. Consequently, validating fiber-assisted treatment for decentralized compact applications requires determining whether its coagulant-saving and separation benefits persist across heterogeneous real wastewaters.

Here, we evaluate an integrated "3-in-1" process that combines fiber-assisted hybrid coagulation–flocculation, solid–liquid separation, and sludge dewatering across contrasting municipal and industrial wastewater matrices (Fig. 1). A residual turbidity target of $\leq$ 25 NTU is used as an operational benchmark to compare conditions and evaluate rapid clarification under conditions relevant to compact treatment[34–37]. Specifically, this study aims to quantify the effect of fibers on i) clarification rate and achievement of the turbidity target, ii) coagulant demand, and iii) the concurrent removal of phosphorus and total organic carbon. The study further assesses the scale-up of fiber-assisted coagulation in a 178-L functional pilot reactor to determine whether rapid clarification can be maintained in a configuration relevant to compact treatment applications.

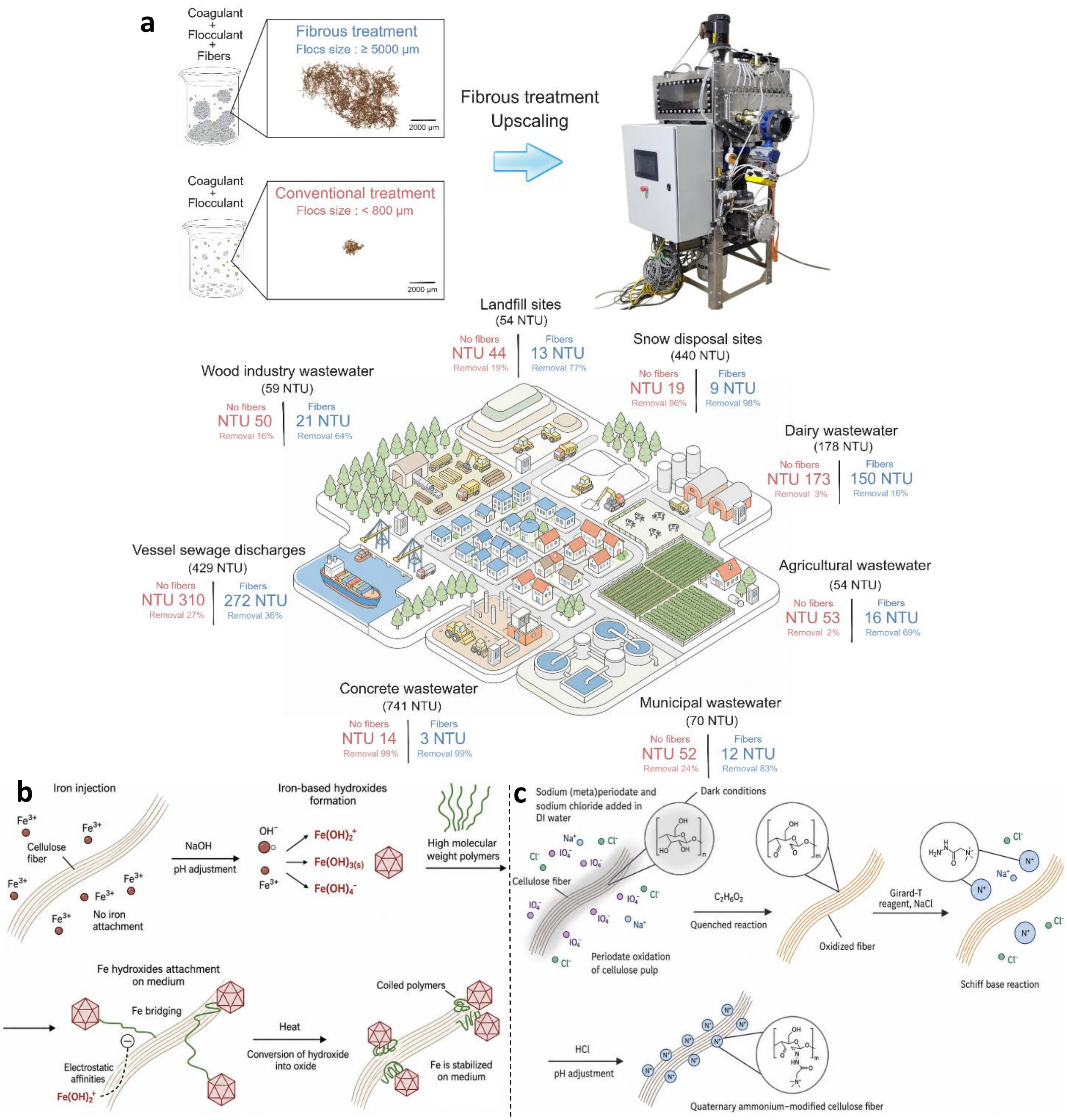

Fig. 1 I Fiber-assisted coagulation–flocculation enables rapid, decentralized clarification and tunable co-benefits. a Conceptual deployment of the fiber-based process for on-site treatment of diverse wastewater streams (e.g., industrial, municipal and landfill-derived). For each matrix, the figure reports representative residual turbidity (NTU) and turbidity removal (%) achieved under rapid separation conditions, comparing conventional coagulation–flocculation (alum + aPAM; red) with fiber-assisted treatment (alum + aPAM + cellulosic fibers; blue). The right-hand panels summarize the main decentralization-relevant outcomes: high-rate treatment (short residence time), reduced operational burden (lower chemical handling/sludge production), and adaptability to influent variability through multiple fiber formulations and co-benefits. The inset illustrates the fiber-induced floc architecture underpinning coarse, low-complexity separation. **b** Schematic of iron-grafting, in which ferric precursors hydrolyze to form iron (oxy)hydroxide domains anchored to the cellulose surface, enabling Fe-mediated interactions during flocculation. **c** Schematic of quaternary ammonium functionalization via periodate oxidation, yielding cationic fibers designed to tune interactions with colloids and organic matter.

Results and Discussion

The addition of super-bridging agents lowers alum demand during rapid settling

The effect of alum dose on clarification by gravity settling was evaluated at two settling times, rapid (30 sec) and extended (3 min), across four contrasting wastewater matrices. Residual turbidity was compared with an operational target of ≤ 25 NTU to distinguish performance achieved. At the lowest alum doses, no clearly discernible flocs were observed, and fibers remained partly dispersed in the supernatant, indicating that sufficient particle destabilization was required before fiber bridging became effective (Fig. 2).

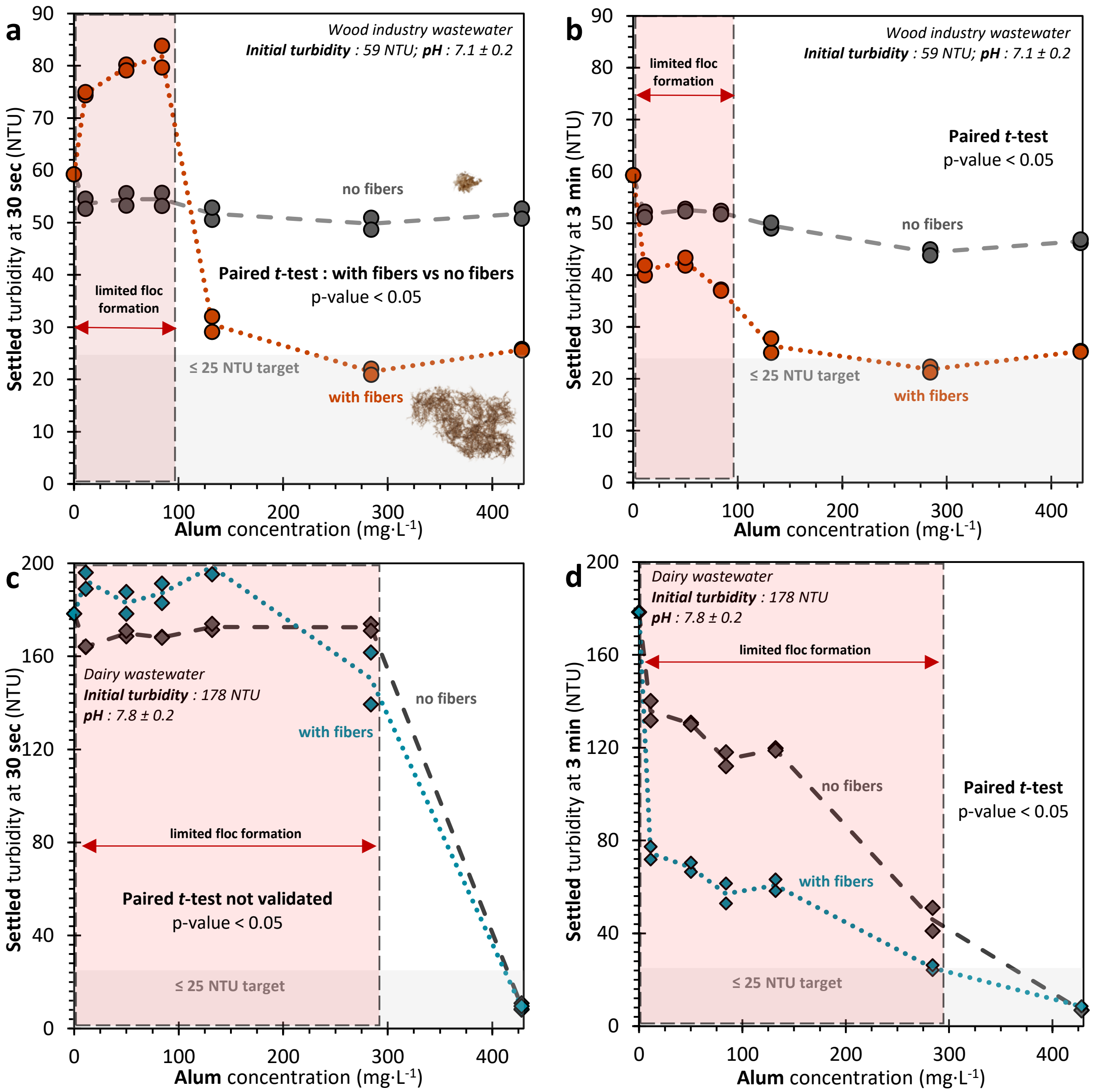

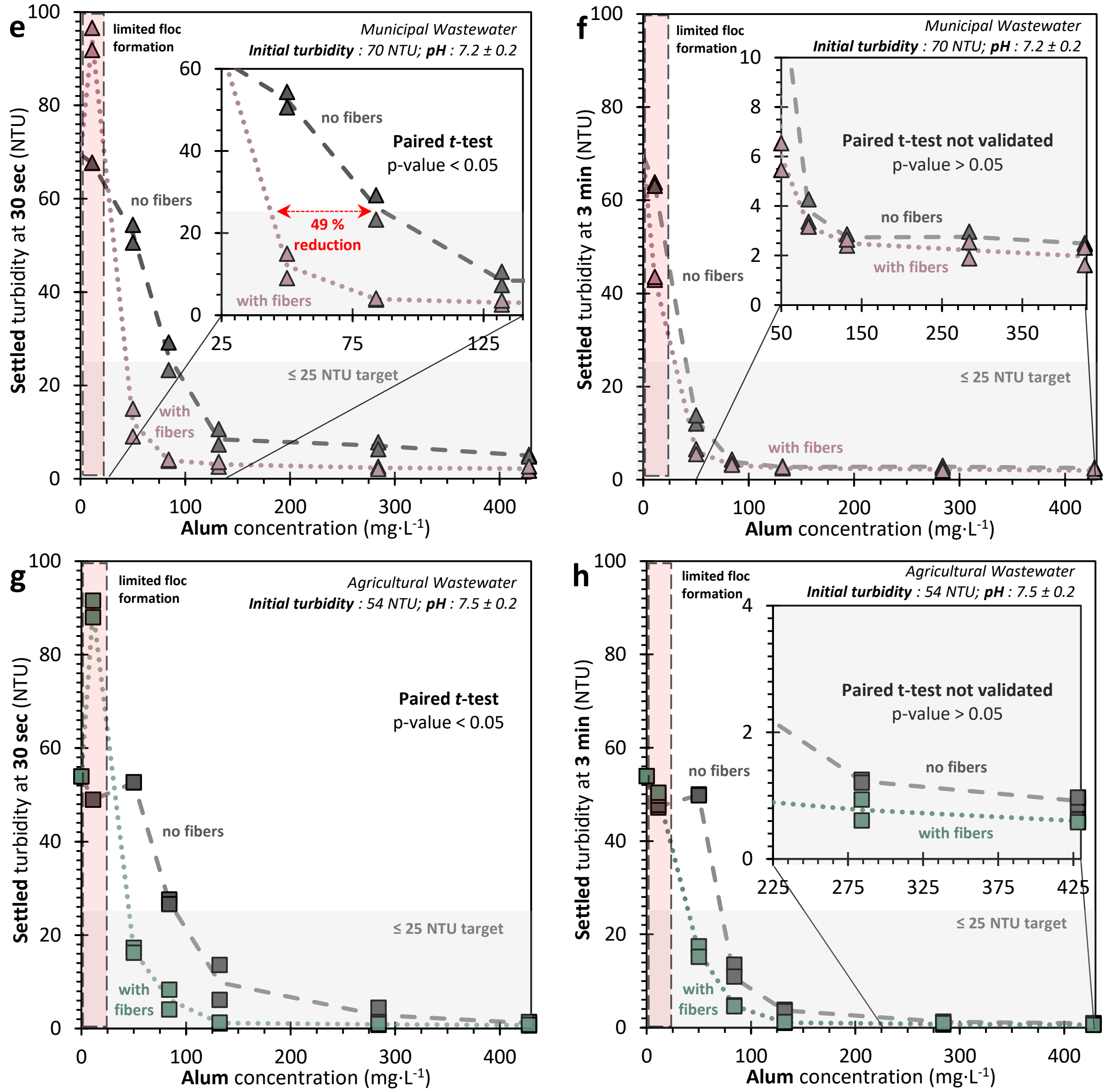

Fig. 2 I Effect of cellulosic fibers on turbidity removal across four real wastewater matrices. Turbidity removal after 30 sec settling for (**a**) wood industry wastewater, (**c**) dairy wastewater, (**e**) municipal wastewater, and (**g**) agricultural wastewater. Turbidity removal after 3 min settling for (**b**) wood industry wastewater, (**d**) dairy wastewater, (**f**) municipal wastewater, and (**h**) agricultural wastewater. Coagulation–flocculation conditions: 11–428 mg-alum·L^{-1}, 1 mg-aPAM·L^{-1}, 200 mg-fibers·L^{-1}, 2 min coagulation, 4 min flocculation, pH 6.8–8.0, 21 °C (**a–h**). Dashed lines are visual guides linking mean values obtained from duplicate experiments. Grey bands indicate the operational target corresponding to a residual turbidity of 25 NTU. The red shaded region indicates conditions where no clearly discernible flocs were observed by visual inspection during jar tests. Unless stated otherwise, differences between fiber-assisted and conventional treatments (no fibers) were statistically significant ($p < 0.05$; **a–h**). Turbidity at 30 sec and 3 min was measured from the same jars (paired measurements).

Once this low-dose regime was exceeded, fiber addition lowered residual turbidity after 30 sec (Fig. 2a; 2c; 2e; 2g) across three matrices. The effect was particularly clear for municipal wastewater, the alum demand at the 25 NTU threshold, estimated using a four-parameter log-logistic model, decreased from 85 mg-alum·L^{-1} (no fibers) to 43 mg-alum·L^{-1} (with fibers), corresponding to a 49% reduction (95% bootstrap CI:

26–69%) and an approximately 2-fold decrease in required dose in 30 sec of settling (equation is provided in Supplementary Materials Eq. S1). In contrast, the dairy wastewater remained difficult to clarify rapidly within the tested dose range, despite a measurable benefit of fiber addition at longer settling time (Fig. 2c, d). After 3 min (Fig. 2b; 2d; 2f; 2h), the difference between treatments became non-significant for the municipal and agricultural wastewaters, whereas it remained significant for the wood and dairy effluents. Fiber addition therefore did not systematically improve the final clarification attainable at high dose and extended settling time. Its main benefit was to accelerate entry into an effective aggregation regime and very short hydraulic residence times, although the magnitude of this benefit remained matrix-dependent.

These contrasting responses indicate that wastewater matrix characteristics influence the kinetics of fiber-assisted aggregation[6–9,32]. This behaviour is consistent with a bridging mechanism that accelerates the growth of larger, dense flocs that are more readily separable by gravity[28,38,39] In particular, the dairy effluent behaviour suggests high colloidal stability associated with proteins and emulsified fats, which likely broadens the dose window required to achieve rapid flocculation[40–42].

Super-bridging agents shifts the floc-size distribution

Floc size is a primary determinant of solid–liquid separation efficiency, particularly in decentralized configurations where footprints are constrained and residence time is short. To examine the structural basis of rapid clarification, floc-size distributions were quantified in municipal wastewater under same alum and polymer conditions with and without fibers (Fig. 3). This matrix was selected as a broadly available representative matrix. Unless otherwise specified, flocculant dosage was maintained at 1 mg·L^{-1} to avoid artefacts related to flocculant limitation, which can reduce fiber-bridging efficiency and restrict floc growth[28,32,43].

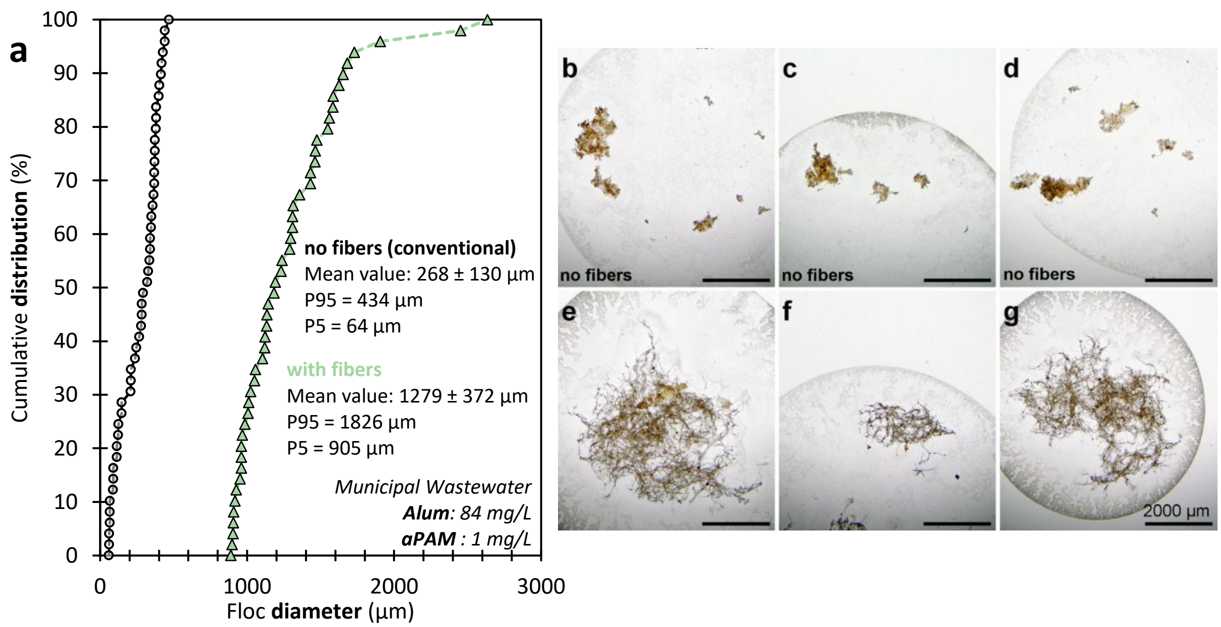

Fig. 3 I Enhanced floc formation through fiber technology. a Cumulative equivalent floc diameter of conventional treatment (no fibers) flocs and fiber treatment flocs. **b-d** Microscope images of conventional flocs. **e-g** Microscope images of fiber-bridged flocs. Treatment conditions: Municipal wastewater 70 NTU, 84 mg-alum·L^{-1}, 1 mg-aPAM·L^{-1}, 200 mg-fibers·L^{-1}, treatment time of 6 min (coagulation 2 min, flocculation 4 min).

Fiber addition shifted the entire floc population toward larger diameters. Mean equivalent diameter increased from 268 to 1,279 µm (maxima exceeding 2633 µm), while P5 increased from 64 to 905 µm and

P95 from 434 to 1,826 µm. On average, flocs were >4.8-fold larger in the fiber-assisted system than in the conventional system. This difference with previous work on super-bridging agents[28,30,32,38,44] can be explained by the use of a non-optimal dose for floc formation and by this first size measurement in a complex matrix. Fiber addition increased both P5 and P95, indicating a population-wide growth rather than a tail effect, and reduced size variability (CV 48% conventional vs 29% fiber-assisted), consistent with a more stable floc-size distribution under rapid-treatment conditions. These trends support a structural mechanism in which fibers act as interparticle connectors and scaffolds that promote network formation and rapid separability[28,36]. Measured sizes likely represent conservative estimates, as floc collection with a wide-mouth pipette inherently limits the diameter of flocs that can be collected.

Screen pressing complements rapid settling

The formation of larger fiber-associated flocs prompted us to evaluate whether they could be mechanically separated rather than relying solely on gravitational settling. Following the settling measurements, the same jars were therefore subjected to screen pressing through a 200-µm mesh (Fig. 4). Because pressing was performed after the 3 min settling measurement, comparison with the 3 min value isolates the additional contribution of the mechanical separation step, whereas comparison with the 30 sec value reflects the combined effect of longer settling and subsequent pressing. (Fig. 4a-d).

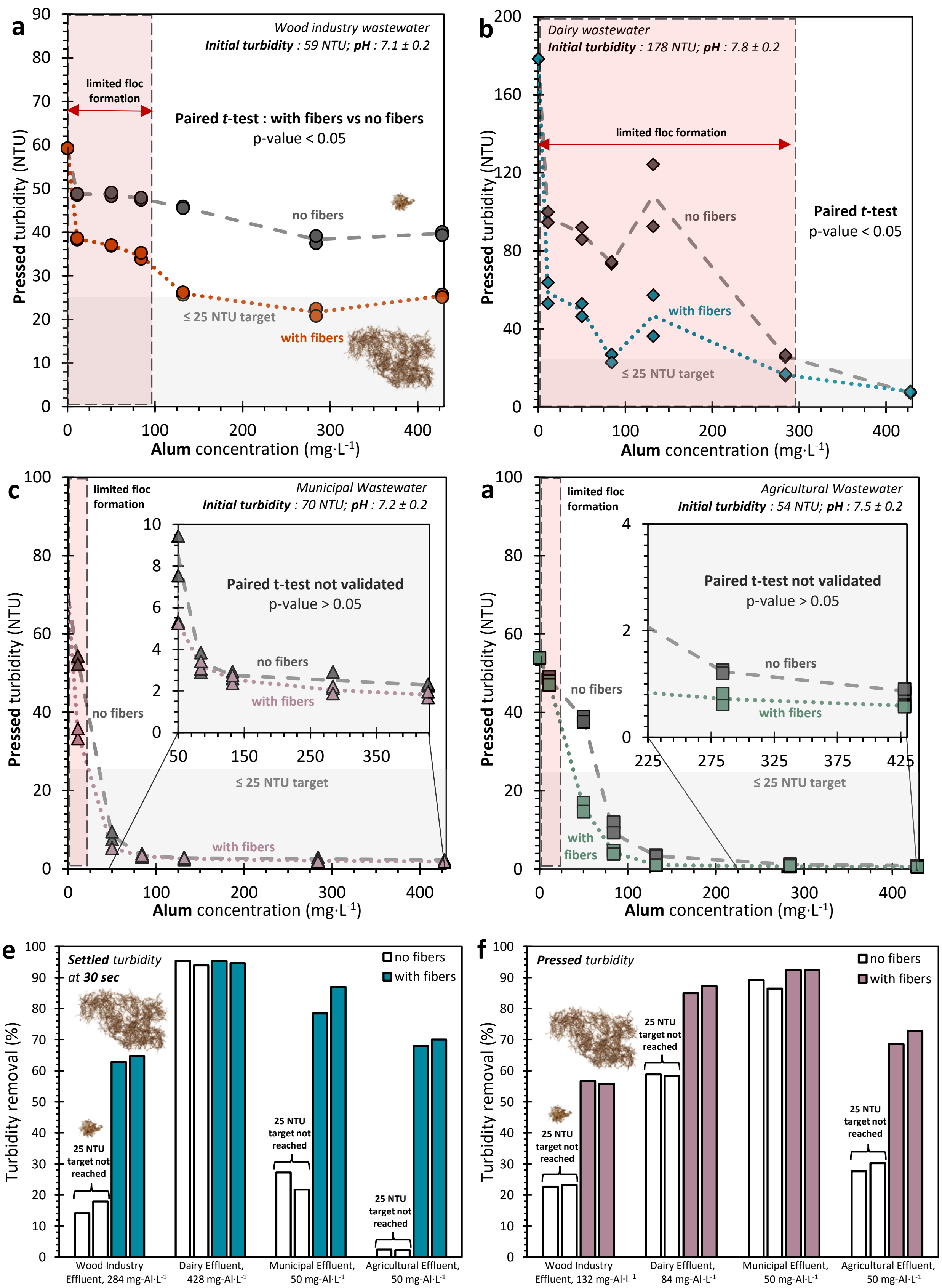
a
Wood industry wastewater
Initial turbidity : 59 NTU; pH : 7.1 ± 0.2
limited floc formation
Paired t-test : with fibers vs no fibers
p-value < 0.05
no fibers
with fibers
≤ 25 NTU target
Pressed turbidity (NTU)
Alum concentration (mg·L-1)
b
Dairy wastewater
Initial turbidity : 178 NTU; pH : 7.8 ± 0.2
limited floc formation
no fibers
with fibers
Paired t-test
p-value < 0.05
≤ 25 NTU target
Pressed turbidity (NTU)
Alum concentration (mg·L-1)
c
limited floc formation
Municipal Wastewater
Initial turbidity : 70 NTU; pH : 7.2 ± 0.2
Paired t-test not validated
p-value > 0.05
no fibers
with fibers
≤ 25 NTU target
Pressed turbidity (NTU)
Alum concentration (mg·L-1)
a
limited floc formation
Agricultural Wastewater
Initial turbidity : 54 NTU; pH : 7.5 ± 0.2
Paired t-test not validated
p-value > 0.05
no fibers
with fibers
≤ 25 NTU target
Pressed turbidity (NTU)
Alum concentration (mg·L-1)
e
Settled turbidity at 30 sec
no fibers
with fibers
25 NTU target not reached
Turbidity removal (%)
Wood Industry Effluent, 284 mg-Al·L-1
Dairy Effluent, 428 mg-Al·L-1
Municipal Effluent, 50 mg-Al·L-1
Agricultural Effluent, 50 mg-Al·L-1
f
Pressed turbidity
no fibers
with fibers
25 NTU target not reached
Turbidity removal (%)
Wood Industry Effluent, 132 mg-Al·L-1
Dairy Effluent, 84 mg-Al·L-1
Municipal Effluent, 50 mg-Al·L-1
Agricultural Effluent, 50 mg-Al·L-1

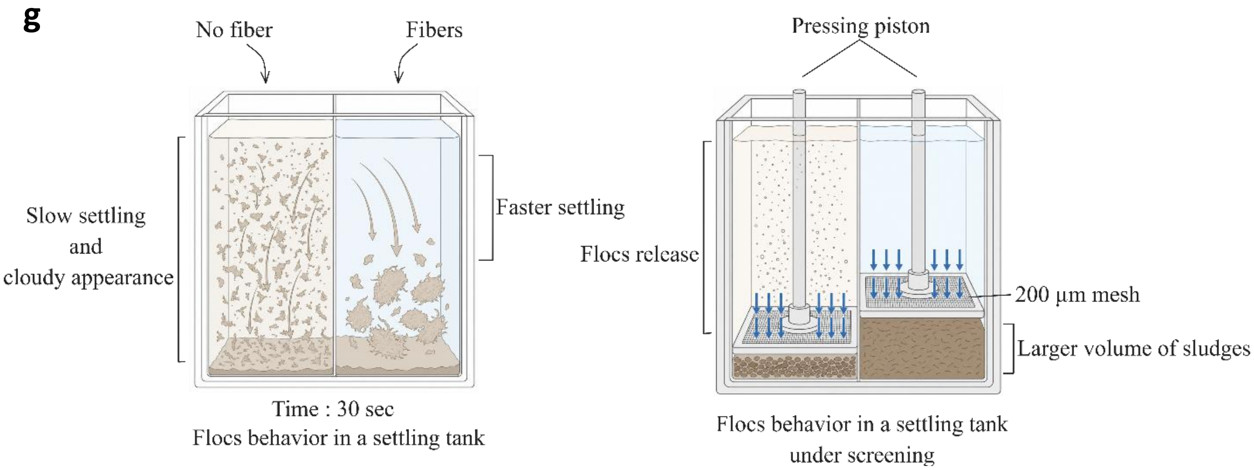

Fig. 4 | Performance of fiber-assisted screening across four real wastewater matrices. Turbidity removal after screening through a 200 μm mesh for (**a**) wood industry wastewater, (**b**) dairy wastewater, (**c**) municipal wastewater, and (**d**) agricultural wastewater. Coagulation–flocculation conditions: 11–428 mg-alum·L^{-1}, 1 mg-aPAM·L^{-1}, 200 mg-fibers·L^{-1}, 2 min coagulation, 4 min flocculation, pH 6.8–8.0, 21 °C. Dashed lines are visual guides linking mean values obtained from duplicate experiments. Grey bands indicate the operational target corresponding to a residual turbidity of 25 NTU. The red shaded region indicates conditions where no clearly discernible flocs were observed by visual inspection during jar tests. Unless stated otherwise, differences between fiber-assisted and conventional treatments (no fibers) were statistically significant ($p < 0.05$; **a–d**). **e** Comparative synthesis of turbidity removal for conventional and fiber-assisted treatments under 30 sec settling, evaluated at the minimum alum dose meeting the 25 NTU target. **f** Comparative synthesis of turbidity removal for conventional and fiber-assisted treatments under pressing, evaluated at the minimum alum dose meeting the 25 NTU target. **g** Schematic of floc behaviour during pressing-assisted dewatering.

Across all matrices and alum doses, final pressed turbidity was on average 37% lower than the 30 sec settling value with fibers and 42% lower without fibers (Fig. 4a-d). These differences include the additional settling time preceding the pressing step. Relative to the immediately preceding 3 min measurement, screen pressing provided a smaller additional turbidity decrease, averaging 11% with fibers and 14% without fibers (Supplementary Table S1). Thus, the difference between settling and pressing depended less on fiber addition itself than on the factorlimiting solid–liquid separation. Previous studies on super-bridging agents showed that increasing floc size can enable screen-based separation because physical retention is less dependent on settling velocity than in gravitational clarification[28,38,39]. For the municipal and agricultural wastewaters (Fig. 4c, d), the minimum tested alum dose required to reach 25 NTU was unchanged between 3 min settling and pressing, indicating that gravitational separation was already sufficient once effective aggregation had been established. A similar absence of further dose reduction was observed for the wood wastewater with fibers (Fig. 4a), suggesting that under these conditions the limiting transition occurred during aggregate formation rather than during subsequent solid–liquid separation.

The dairy wastewater exhibited a different separation regime (Fig. 4b). With fibers, the minimum tested alum dose meeting the 25 NTU target decreased from 428 mg-alum·L^{-1} after 3 min settling to 84 mg-alum·L^{-1} after pressing, corresponding to an 80% reduction (Fig. 4e,f). Thus, at intermediate alum doses, fiber-assisted aggregation produced aggregates that could be retained mechanically even though gravitational separation remained insufficient within 3 min. This distinction is consistent with previous super-bridging studies showing that screen retention can compensate for limited settling when aggregates have formed but remain poorly separated by gravity[28,38,39]. It also extends previous observations obtained with simpler water matrices by showing that the relative value of settling and mechanical retention depends strongly on wastewater characteristics. Importantly, pressing did not appreciably deteriorate effluent quality under fiber-assisted conditions: increases relative to the preceding 3 min turbidity were infrequent and limited (≤0.7 NTU). Screen pressing is therefore most useful when flocs are large enough to be physical retained but settle slowly for efficient gravity separation (illustrated in Fig. 4g).

Clarification benefits vary across real wastewater matrices

To assess whether the fiber-associated clarification benefit extended beyond the four matrices investigated in detail, performance was compiled across 14 industrial, municipal and landfill-derived wastewater conditions spanning initial turbidities from 15 to 4500 NTU and a broad range of organic contents (Supplementary Tables S2 and S3). Final turbidity was lower with fibers in all tested conditions, although the relative improvement varied from 5 to 81%. Large gains were observed for chemically distinct waters, including concrete manufacturing wastewater (81%), municipal wastewater (up to 77%), landfill-derived waters (up to 75%), agricultural wastewater (68%) and wood-industry wastewater (57%). The fiber benefit was therefore not restricted to a specific wastewater type or initial turbidity range, but its magnitude remained condition dependent.

Municipal wastewater experiments further illustrate this dependence on operating conditions (Fig. 5). Increasing polymer dosage improved clarification in both treatments, whereas fiber addition produced its strongest advantage under short settling times, reducing residual turbidity to ~3 NTU at 0.6–1.0 $mg\cdot L^{-1}$ polymer compared with ~7–10 NTU without fibers (Fig. 5a). The smaller difference after 3 min settling, together with the lower residual TSS observed (minimum of 1 $mg\text{-}TSS\cdot L^{-1}$) with fibers (Fig. 5b,c), indicates that fibers primarily accelerate the formation of rapidly separable aggregates. This structural effect was further demonstrated by coarse screening through a 2000-µm mesh: alum or alum–aPAM alone produced aggregates that were poorly retained, whereas fiber-assisted treatment maintained low turbidity across the alum range tested (Fig. 5d). These results suggest that the variability observed across real wastewaters reflects the combined influence of particle destabilization, polymer availability, colloidal characteristics and separation conditions rather than wastewater category, initial turbidity or TOC alone [28,38,43,45,46]. Despite this variability, the persistence of a positive fiber effect across heterogeneous matrices supports fiber-assisted flocculation as a flexible strategy for high-rate clarification.

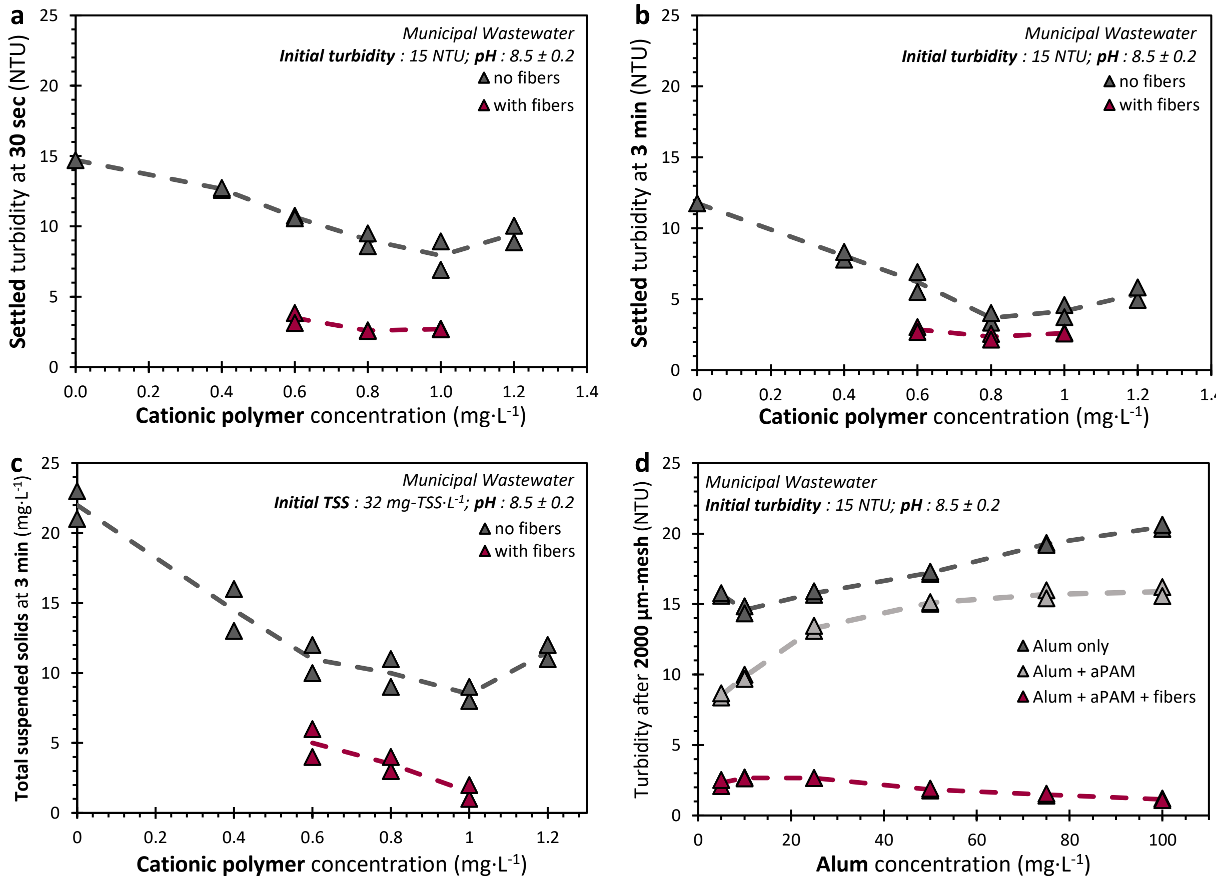

Fig. 5 I Effect of polymer dosage and coarse screening on fiber-assisted clarification of municipal wastewater. Residual turbidity after **a** 30 sec and **b** 3 min settling as a function of cationic polymer concentration, comparing conventional treatment without fibers and fiber-assisted treatment. **c** Total suspended solids (TSS) after 3 min settling under the same polymer-dose conditions. **d** Turbidity after separation through a 2000-µm mesh at increasing alum concentrations for alum alone, alum + aPAM, and alum + aPAM + fibers. Municipal wastewater had an initial turbidity of 15 NTU and a pH of 8.5 ± 0.2. Dashed lines are visual guides connecting mean values obtained from replicate experiments.

Fiber surface chemistry adds contaminant capture beyond structural clarification

Two alum doses were selected to probe process robustness and the ability of fibers to shift the operating window: an baseline dose, defined as a dose that meets the turbidity target without fibers (84 mg-alum·L^{-1}), and a reduced-dose, defined as the minimum dose that meets the target with fibers (50 mg-alum·L^{-1}) (Fig. 2). This contrast enables assessment of (i) the process tolerance to reduced coagulant input and (ii) the extent to which fiber surface chemistry modulates performance beyond clarification alone (Fig. 6).

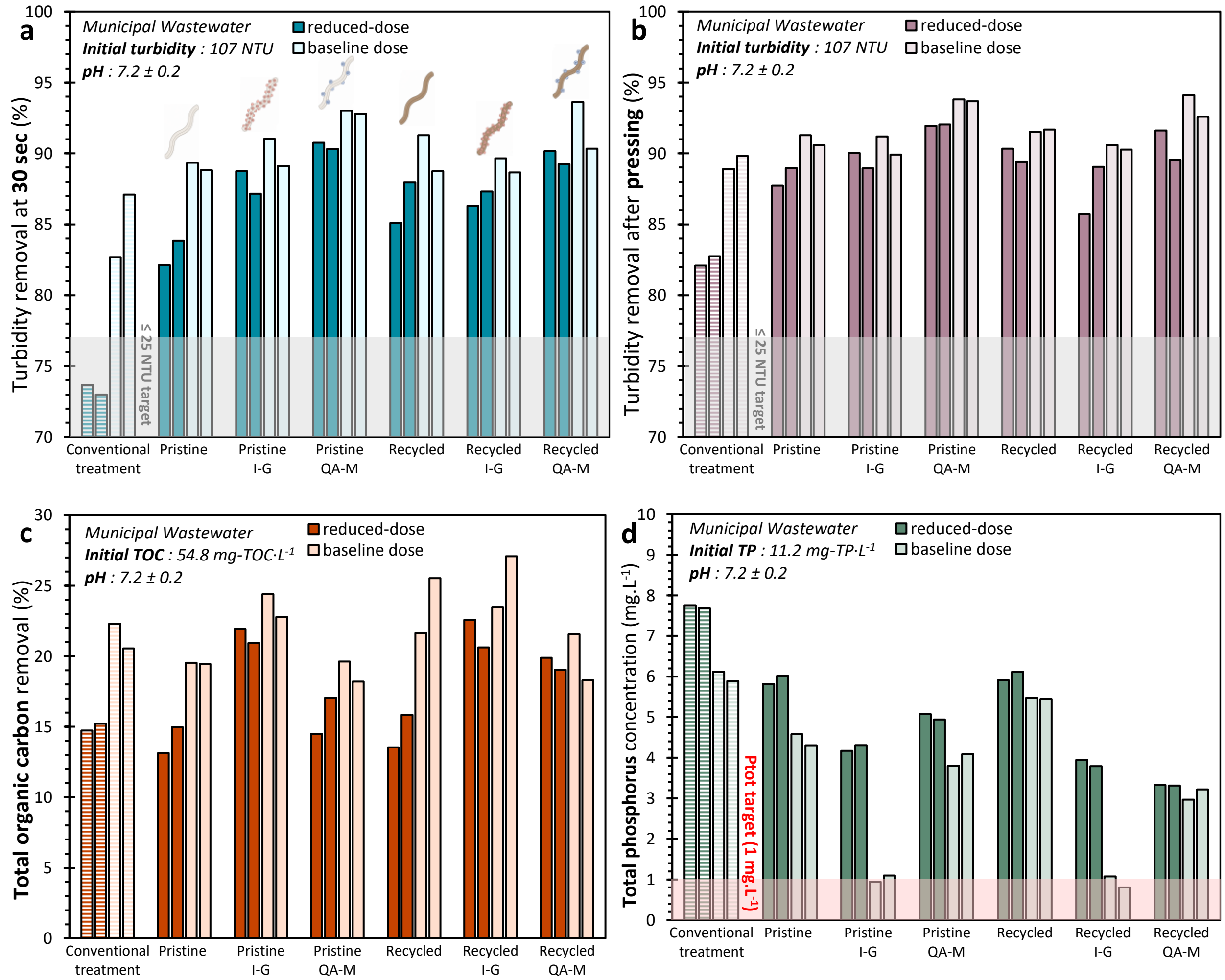

Fig. 6 I Performance of pristine and recycled functionalized cellulosic fibers in municipal wastewater under suboptimal and optimal coagulation regimes. Municipal wastewater (initial turbidity 107 NTU, pH 7.2 ± 0.2) was treated using the conventional coagulation–flocculation baseline (no fibers) or fiber-assisted treatment with pristine or recycled cellulose fibers (unmodified, **I-G**: iron-grafted, or **QA-M**: quaternary ammonium–modified). For each formulation, performance was evaluated under suboptimal and optimal alum dosing conditions (defined in Fig. 2). **a** Turbidity removal after 30 sec settling. **b** Turbidity removal after coarse screening (200 µm). The grey bands in (**a,b**) indicate the minimum turbidity removal required to reach the operational target of ≤ 25 NTU. **c** Total organic carbon (TOC) removal (initial TOC 54.8 mg-TOC·L⁻¹, pH 7.2 ± 0.2), after 6 minutes of treatment and 3 minutes of settling. **d** Residual total phosphorus (TP) concentration (initial TP 11.2 mg-TP L⁻¹, pH 7.2 ± 0.2), after 6 minutes of treatment and 3 minutes of settling. The red shaded band in **d** indicates a reference discharge limit of 1 mg-TP·L⁻¹ (Québec municipal facilities)[47]. Bars represent duplicate experiments.

Fiber addition converts clarification of a municipal effluent into a process compatible with very short contact and separation times (reduction in contact time is shown in the Supplementary Fig. S2). Under reduced-dosethe conventional treatment does not achieve the turbidity reduction required to meet ≤ 25 NTU after 30 sec (Fig. 6a), whereas all fiber formulations tested—pristine and recycled, modified and unmodified (characterization provided in the Supplementary Table S4) exceed this threshold. This indicates that, at low coagulant dose, the limiting factor is not solely charge neutralization but the ability to rapidly build a separable floc architecture; fibers act here as a re-structuring lever through bridging, accelerating larger floc formation and reducing sensitivity to operating conditions. Underbaseline dose, the fiber effect remains positive but the relative gain narrows, consistent with a regime in which conventional coagulation is already sufficiently effective and fibers primarily enhance and stabilize performance.

Introducing mechanical separation via pressing through a 200-µm mesh provides an additional safeguard (Fig. 6b). Screening allows the conventional treatment to reach the turbidity threshold even at low dose, confirming that mechanical action can compensate for gravity-separation limitations under rapid-treatment conditions. However, fibers retain a clear advantage: they maintain consistently high removal and, importantly, reduce dependence on coagulant dose and settling rate. These results also indicate an absence of measurable re-entrainment during screening, suggesting that coarser screens could potentially be used under fiber-assisted treatment without compromising effluent turbidity.

Beyond the overall fiber effect, both the fiber source (pristine vs recycled) and surface chemistry (unmodified, iron-grafted, quaternary ammonium–modified) influence performance, but in indicator-specific ways. For turbidity, most formulations converge toward high removals, indicating that clarification is governed primarily by the structural role of fibers, enhancing floc size and cohesion, rather than by a specific surface functionality. This robustness suggests that recycled material can retain an intensification function comparable to pristine fiber, strengthening the process rationale in terms of sustainability[48–50]. Nonetheless, differences among formulations become more apparent when comparing reduced-dose versus baseline dose, implying that surface chemistry may widen or narrow the operating window, for instance through interactions with stabilized colloids, organic matter, or metal coagulant species.

TOC removal remains moderate (Fig. 6c), as expected for a process whose primary objective is rapid clarification rather than removal of the dissolved fraction. In this context, the decrease in TOC mainly reflects capture of the particulate/colloidal fraction associated with turbidity, rather than removal of dissolved organics[51]. Still, the variability among fibers and the improvement observed under baseline dose for some formulations suggest that fiber type can influence organic capture, either indirectly via a denser floc architecture[52], or through specific interactions (electrostatic) with particulate organic fractions[43]. Overall, this performance is consistent with a pre-treatment role: reducing load and stabilizing influent quality upstream of a downstream unit (biological treatment or adsorption/oxidation), with potential benefits for fouling control, hydraulic variability, and the energy demand of subsequent processes.

The total phosphorus results reveal a distinct outcome (Fig. 6d): iron functionalization confers a markedly enhanced capacity for total phosphorus removal, yielding residual concentrations approaching or below 1 mg-TP L^{-1} under baseline dose. Under this condition, iron grafting reduced residual TP from 4.44 to 1.02 mg-TP·L^{-1} for white fibers and from 5.46 to 0.94 mg-TP·L^{-1} for brown fibers, despite nearly identical turbidity removal between grafted and ungrafted formulations. This decoupling between turbidity and phosphorus removal points to an additional removal pathway associated with the iron functionality, such as phosphate adsorption/complexation onto ferric sites and/or co-precipitation with aluminum hydroxides formed during coagulation[52,53]. In other words, two functions can be decoupled: (i) a “structural” fiber that rapidly generates separable flocs and secures turbidity control, and (ii) a “functional” fiber (iron-grafted) that adds a targeted co-benefit for nutrient removal. From a decentralization perspective, this modularity enables material selection to be tailored not only to settleability but also to local priorities (e.g., phosphorus control) without requiring additional treatment units.

Pilot-scale implementation and preliminary performance under high-rate operation

To evaluate process translatability beyond jar tests, a 178-L pilot reactor was engineered and operated as an integrated module combining mixing, rapid solid–liquid separation and sludge handling (Fig. 7a). The unit incorporates an internal filter wall that separates clarified water from a concentrated solids stream, a dedicated sludge outlet for downstream thickening/secondary filtration, and an in-situ cleaning system (schematized in Fig. 7b-d) consistent with operational requirements for compact, decentralized units. Pilot operation was conducted under controlled mixing conditions (coagulation at 115 rpm, flocculation at 80 rpm) and short-cycle handling, with reactor filling completed in ~30 sec and draining in ~1 min. The cleaning architecture comprises nine nozzles supplied at 95 psi on an 800 µm mesh, providing a practical pathway for maintenance by design (Fig. 7c, d), although long-term fouling metrics (e.g., pressure drop, flux decay) were not quantified in this preliminary campaign.

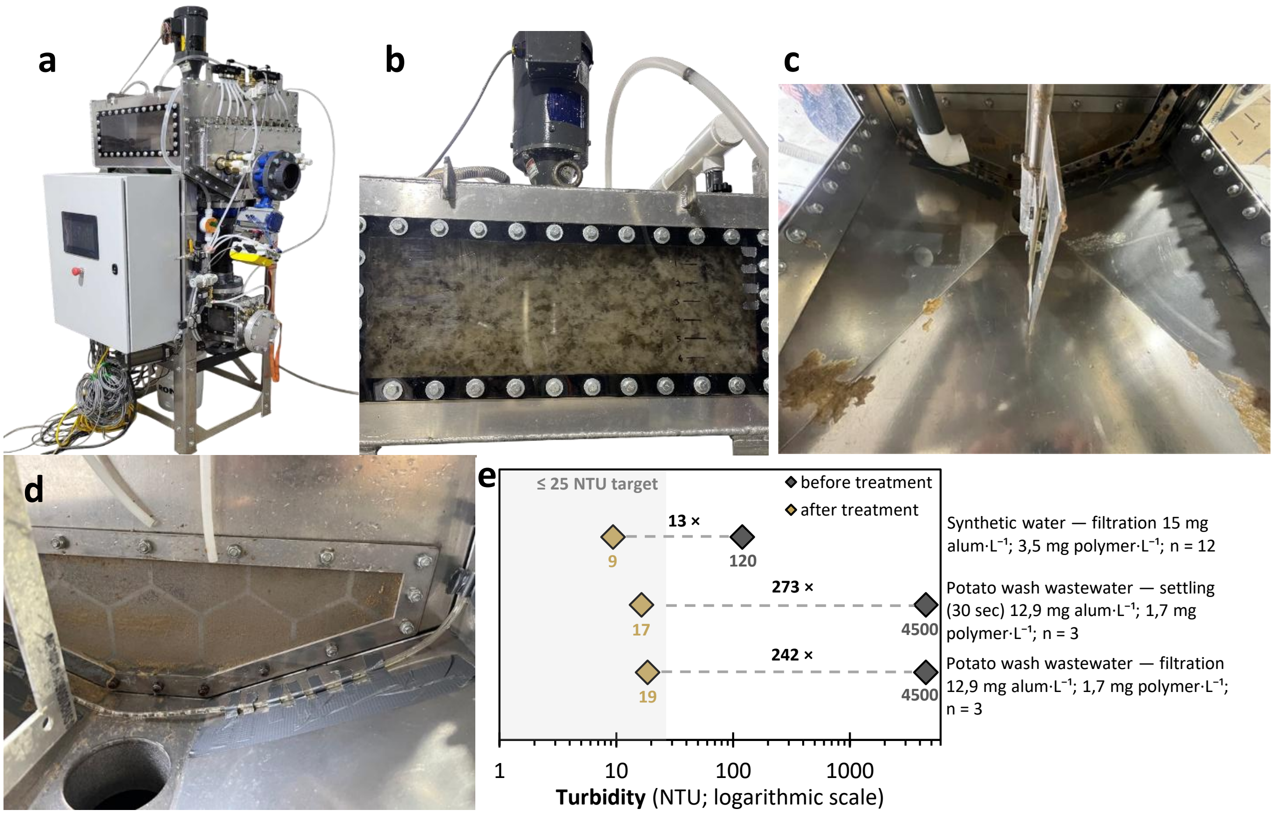

Fig. 7 I Pilot-scale reactor for fiber-assisted coagulation–flocculation and integrated solid–liquid separation, a Photograph of the 178-L pilot unit with integrated mixing and control system. **b** View through the inspection window during operation. **c** Internal view of the reactor showing the solids collection zone and sludge withdrawal region. **d** Internal filter wall after operation, illustrating solids capture on the separation surface. **e** Summary of operating conditions (treated volume, alum, polymer and fibre dosages), number of replicates, and average initial and final turbidity for the pilot reactor. Turbidity outcomes are reported for rapid settling (30 sec) and filtration modes. The reduction factor is defined as $NTU_{initial}/NTU_{final}$. All pilot tests were conducted in fibre-assisted mode. Operating conditions for the pilot campaigns were 115 rpm during coagulation and 80 rpm during flocculation; the cleaning system comprised nine nozzles supplied at 95 psi.

Preliminary clarification results are shown in Fig. 7e. Under constant fiber dosing, the pilot achieved reproducible clarification on synthetic wastewater in filtration mode (n = 12), with turbidity decreasing from 120 to 9 NTU (reduction factor 13×, corresponding to 92.2% removal). A first real-matrix validation on potato wash wastewater, a highly loaded stream (initial turbidity 4500 NTU), demonstrated consistent attainment of the operational target ≤ 25 NTU (n = 3) under high-rate conditions. Final turbidity averaged 17 NTU after 30 sec settling (reduction factor 273, 99.6% removal) and 19 NTU in filtration mode (reduction factor 242, 99.6% removal). The small difference between settling and filtration outcomes for this matrix suggests that, under these operating conditions, both separation pathways provide effective clarification and that the internal separation step does not induce measurable particle re-entrainment. In line with the bench-scale observation that fiber-assisted treatment produces robust large flocs amenable to coarse separation, these pilot observations motivate future exploration of coarser filter-wall geometries to further reduce hydraulic resistance and simplify maintenance, while explicitly quantifying solids capture, head loss and cleaning frequency.

These pilot results should be interpreted as an engineering feasibility and operability demonstration rather than a head-to-head performance comparison. The campaign was conducted in fiber-assisted mode only, without a no fiber baseline at pilot scale, and real wastewater testing remains limited (n = 3 for potato wash wastewater). Nonetheless, the operation of an integrated module combining clarification, solids withdrawal and in situ cleaning, together with the preliminary achievement of ≤ 25 NTU for a highly turbid real wastewater, provides an initial engineering translation of fiber-assisted clarification beyond jar-scale experiments.

Conclusion

This study demonstrates that engineering floc architecture with renewable cellulosic fibers can convert conventional alum–polymer coagulation–flocculation into a high-rate, low-complexity clarification strategy aligned with decentralized and hybrid wastewater systems. Across contrasting real matrices, fibers enabled a transition from poorly separable regimes to rapidly separable flocs, allowing the operational target ≤ 25 NTU to be met under 30 sec settling and/or coarse screening. This enhanced clarification was also reflected in solids removal, with residual TSS concentrations reaching as low as ~1 mg-TSS·L^{-1}. The reduction in coagulant demand is practically consequential: for municipal wastewater, the modelled dose-to-target at 25 NTU decreased from 85 to 43 mg-alum·L^{-1} (49% reduction, 95% bootstrap CI 26–69%), while floc-diameter measurements confirmed the mechanistic basis of intensification (mean diameter 268 to 1279 µm, > 4.8-fold; reduced size variability). A multi-matrix dataset further shows that fiber benefits persist across diverse real wastewaters, with performance modulated by matrix complexity (e.g., stabilized, protein/fat-rich waters remain more challenging under rapid conditions). Moreover, the fiber support is tunable: pristine/recycled fibers delivered robust turbidity control, whereas iron-grafted fibers introduced a distinct nutrient-capture function, reducing residual total phosphorus to ~1 mg-TP·L^{-1} under optimal dosing, decoupling "structural" clarification from "functional" co-benefits.

A 178-L pilot reactor integrating an internal filter wall, sludge withdrawal and in situ cleaning achieved strong preliminary clarification (synthetic water, n=12; potato wash wastewater, n=3), providing an engineering translation step. While pilot testing lacked a no fiber baseline and long-term fouling metrics, these results establish a deployable process architecture and motivate next-stage campaigns that quantify head loss, cleaning frequency, solids capture and full comparative performance under variable real influents. Overall, fiber-enabled coagulation–flocculation offers a practical route to compact, resilient pre-treatment that can reduce chemical burden and expand operational flexibility in decentralized water management.

Materials and methods

Chemicals and materials

Jar tests were conducted to emulate a compact, low-complexity treatment configuration compatible with decentralized deployment (e.g., without granular filtration). The anionic polyacrylamide tested (Hydrex 3511) was supplied by Veolia, and the cationic polyacrylamide (C-498) was supplied by Kemira Water Solutions Canada Inc.; all solutions and suspensions were prepared using reverse-osmosis (RO) water. Fiber suspensions were prepared as described elsewhere by dispersing 2.5 g of dry fibers in 500 mL of RO water (Ninja blender, for 30 sec). Ferric chloride (PIX 311) was used as the iron precursor for fiber grafting; this reagent was selected for its favourable hydrolysis behaviour, enabling the formation of stable iron (oxy)hydroxide domains that can enhance contaminant adsorption and promote particle–fiber bridging during flocculation[53]. Quaternary ammonium–functionalized cellulose fibers were prepared using an adapted protocol previously reported for periodate oxidation followed by quaternary ammonium derivatization with Girard's reagent T (2-hydrazinyl-2-oxoethyl trimethylammonium chloride; Thermo Fisher Scientific), as detailed in the cited literature[30,54].

Jar tests

Jar-test coagulation–flocculation experiments were conducted to systematically evaluate the performance of different treatment combinations involving coagulant, polymers and cellulosic fibers. Experiments were carried out in 250 mL glass beakers placed on a Corning magnetic stirring plate, with a mixing speed of 200 rpm. The stirring system used cross-shaped magnetic stir bars (3.5 cm × 3.5 cm), and all tests were performed at room temperature (~22 °C).

Six fiber types were investigated: (i) pristine fibers, (ii) recycled fibers, (iii) pristine iron-grafted fibers, (iv) recycled iron-grafted fibers, (v) pristine quaternary ammonium–modified fibers, and (vi) recycled quaternary ammonium–modified fibers. Cellulosic fibers (eucalyptus hardwood cellulose; Sigma, NISTRM8496) and recycled cardboard fibers were prepared by dispersing 2.5 g of dry material in 500 mL of RO water and homogenizing for 30 sec to obtain a uniform suspension. Synthesis procedures for the iron-grafted and quaternary ammonium–modified fibers followed previously published protocols[55,53]. The flocculant used throughout was anionic polyacrylamide (aPAM). A fresh aPAM stock solution (500 $mg\cdot L^{-1}$) was prepared by dissolving 50 mg of aPAM powder in 100 mL of RO water under magnetic stirring for 15 min. Because polyacrylamide can degrade over time–potentially decreasing molecular weight and flocculation efficiency–freshly prepared polymer solutions were used to ensure consistent performance.

Each experiment started with addition of the coagulant, an aluminum sulfate solution (ALS; alum), to the test matrix, followed by 2 min of rapid mixing for coagulation. A range of ALS concentrations was tested: 11, 50, 84, 132, 284 and 428 $mg\cdot L^{-1}$. After coagulation, fibers and the first half of the polymer dose were added simultaneously to reach final concentrations of 200 mg-fibers$\cdot L^{-1}$ and 1 mg-aPAM$\cdot L^{-1}$, respectively. The total aPAM dose was split into two equal aliquots to reduce the risk of polymer desorption and reconfiguration[56,57]. The second half was added after 2 min of mixing, followed by an additional 2 min of flocculation mixing. After flocculation, samples were allowed to settle for 30 sec or 3 min, and turbidity was measured at both time points using a turbidimeter.

In addition to conventional settling, a mechanical screening step was introduced to emulate compact sludge dewatering and to further evaluate separation performance. Screening was performed using a filter press fitted with a 200 μm mesh. The filtrate collected after screening was analysed for turbidity, total organic carbon removal, and total phosphorus. All conditions were tested in duplicate, and at least three analytical measurements were performed per sample to minimize analytical variability. The full protocol was also run without fibers to provide a conventional-treatment baseline.

Turbidity, total organic carbon and total phosphorus measurement

Turbidity was measured according to Standard Method 2130B using a Hach 2100N turbidimeter. Total organic carbon (TOC) concentrations were determined following Standard Method 5310C with a Sievers 5310c TOC analyzer (GE Water). Total suspended solids (TSS) were determined by the Standard Method 2540D with glass microfibre filters (pore size 0.7 μm, GE Healthcare Life Sciences, Whatman). Total phosphorus (TP) was measured in accordance with Standard Method 4500P, based on persulfate digestion to convert all phosphorus forms to orthophosphate, followed by colorimetric determination of orthophosphate using the ascorbic acid method (Standard Method 4500-P E). Digested samples were analyzed spectrophotometrically using a Cary 60 UV-Vis.

Authorship contribution statement

Mathieu Verhille: Conceptualization, Methodology, Validation, Formal analysis, Investigation, Data Curation, Visualization, Writing - Original Draft.
Emilia Tognetty: Validation, Formal analysis, Investigation, Data Curation, Writing - Original Draft, Visualization.
Manel Mebarki: Validation, Formal analysis, Investigation, Data Curation, Writing - Original Draft, Visualization.
Lovenie Victor: Validation, Investigation, Data Curation.
Masashi Kaneda: Validation, Investigation, Data Curation.
Owen Armstrong: Validation, Investigation, Data Curation.
Nathalie Tufenkji: Validation, Review & Editing.
Mathieu Lapointe: Conceptualization, Methodology, Validation, Formal analysis, Investigation, Resources, Data Curation, Writing, Review & Editing, Visualization, Supervision, Project administration, Funding acquisition.

Declaration of Competing Interests

M.L. and N.T. have applied for a patent on the use of fiber-based materials for water treatment. The remaining authors declare no competing interests.

Acknowledgments

The authors acknowledge the assistance provided by Water Engineering and Environmental Processes Laboratory (LGEPE) at École de technologie supérieure (University of Québec). The authors also acknowledge the financial support from the Canada Research Chairs program (CRC-2022-00274), the Natural Sciences and Engineering Research Council of Canada (NSERC) Discovery Grants program (RGPIN-2023-03486), the ministère de l'Agriculture, des Pêcheries et de l'Alimentation (MAPAQ) and the ministère de l'Environnement, de la Lutte contre les changements climatiques, de la Faune et des Parcs (MELCCFP) (Plan national de l’eau), and the ministère de l’Économie, de l’Innovation et de l’Énergie (MEIE, PSO program; AXE – 0446).

References

1. Marcogliese, D. J. *et al.* Effects of a major municipal effluent on the St. Lawrence River: A case study. *Ambio* **44**, 257–274 (2015).
2. Keller, J. Why are decentralised urban water solutions still rare given all the claimed benefits, and how could that be changed? *Water Res. X* **19**, 100180 (2023).
3. Garrido-Baserba, M. *et al.* Using water and wastewater decentralization to enhance the resilience and sustainability of cities. *Nat. Water* **2**, 953–974 (2024).
4. *Source Separation and Decentralization for Wastewater Management*. (IWA Publishing, 2013).
5. Garrido-Baserba, M. *et al.* The third route: A techno-economic evaluation of extreme water and wastewater decentralization. *Water Res.* **218**, 118408 (2022).
6. Eddy, I. M. &, Tchobanoglous, G., Burton, F. & Stensel, H. D. *Wastewater Engineering: Treatment and Reuse*. (McGraw-Hill Science/Engineering/Math, Boston, Mass., 2003).
7. Fiorentino, A. *et al.* Impact of industrial wastewater on the dynamics of antibiotic resistance genes in a full-scale urban wastewater treatment plant. *Sci. Total Environ.* **646**, 1204–1210 (2019).
8. Iloms, E., Ololade, O. O., Ogola, H. J. O. & Selvarajan, R. Investigating Industrial Effluent Impact on Municipal Wastewater Treatment Plant in Vaal, South Africa. *Int. J. Environ. Res. Public. Health* **17**, 1096 (2020).
9. Mekuria, D. M., Kassegne, A. B. & Asfaw, S. L. Assessing pollution profiles along Little Akaki River receiving municipal and industrial wastewaters, Central Ethiopia: implications for environmental and public health safety. *Heliyon* **7**, e07526 (2021).
10. Mikosz, J. Determination of permissible industrial pollution load at a municipal wastewater treatment plant. *Int. J. Environ. Sci. Technol.* **12**, 827–836 (2015).

11. Tauber, J., Flesch, B., Parravicini, V., Svardal, K. & Krampe, J. Influence of road salt thawing peaks on the inflow composition and activated sludge properties in municipal wastewater treatment. *Water Sci. Technol.* **84**, 314–322 (2021).
12. Collivignarelli, M. C., Caccamo, F. M., Bellazzi, S., Abbà, A. & Bertanza, G. Assessment of the Impact of a New Industrial Discharge on an Urban Wastewater Treatment Plant: Proposal for an Experimental Protocol. *Environments* **10**, 108 (2023).
13. Rai, S. *et al.* Cost and Carbon Implications of Industrial Organic Load Reduction across Water Resource Recovery Facility Typologies. *Environ. Sci. Technol.* **60**, 3633–3645 (2026).
14. Bourgin, M. *et al.* Evaluation of a full-scale wastewater treatment plant upgraded with ozonation and biological post-treatments: Abatement of micropollutants, formation of transformation products and oxidation by-products. *Water Res.* **129**, 486–498 (2018).
15. Paśmionka, I. B. *et al.* Influence of COD in Toxic Industrial Wastewater from a Chemical Concern on Nitrification Efficiency. *Int. J. Environ. Res. Public. Health* **19**, 14124 (2022).
16. Del Nery, V. *et al.* Long-term operating performance of a poultry slaughterhouse wastewater treatment plant. *Resour. Conserv. Recycl.* **50**, 102–114 (2007).
17. Sharghi, E. A. & Davarpanah, L. Optimization of chemical coagulation–flocculation process of detergent manufacturing plant wastewater treatment for full scale applications: a case study. *Desalination Water Treat.* **262**, 38–53 (2022).
18. Xi, J. *et al.* Enhanced nutrient removal from stormwater runoff by a compact on-site treatment system. *Chemosphere* **290**, 133314 (2022).
19. Sang, Y. *et al.* Pilot-scale microsand-ballasted flocculation of wastewater: turbidity removal, parameters optimization, and mechanism analysis. *Environ. Sci. Pollut. Res.* **29**, 32161–32170 (2022).

20. Nguyen, T. A., Nguyen, H. D., Schmalz, B. & Tran, L. L. Coagulation/floculation as a key unit in the decentralized surface water treatment systems in upland rural areas of Vietnam: Results from a lab scale to a pilot scale system. *Process Saf. Environ. Prot.* **194**, 1194–1205 (2025).
21. Ismail, I. M., Fawzy, A. S., Abdel-Monem, N. M., Mahmoud, M. H. & El-Halwany, M. A. Combined coagulation flocculation pre treatment unit for municipal wastewater. *J. Adv. Res.* **3**, 331–336 (2012).
22. Sher, F., Malik, A. & Liu, H. Industrial polymer effluent treatment by chemical coagulation and flocculation. *J. Environ. Chem. Eng.* **1**, 684–689 (2013).
23. Wang, B.-Y., Chen, Z.-L., Zhu, J., Shen, J.-M. & Han, Y. Pilot-scale fluoride-containing wastewater treatment by the ballasted flocculation process. *Water Sci. Technol. J. Int. Assoc. Water Pollut. Res.* **68**, 134–143 (2013).
24. Ho, Q. N., Fettweis, M., Spencer, K. L. & Lee, B. J. Flocculation with heterogeneous composition in water environments: A review. *Water Res.* **213**, 118147 (2022).
25. Moreira, V. R. *et al.* Restrictions in water treatment by conventional processes (coagulation, flocculation, and sand-filtration) following scenarios of dam failure. *J. Water Process Eng.* **51**, 103450 (2023).
26. He, W., Luo, J., Wu, Y., Luo, T. & Tang, C. Differently charged polyacrylamides (PAMs) significantly affect adsorption affinity and associated floc growth behaviors during ballasted flocculation: Performance and mechanism. *Sep. Purif. Technol.* **329**, 125279 (2024).
27. He, W., Yang, Z., Fang, K., Luo, J. & Zhang, J. Mechanistic insights into molecular weight-driven and hydrophobicity-mediated effects on floc growth properties during two-stage ballasted flocculation for organics removal. *Sep. Purif. Technol.* **395**, 137734 (2026).
28. Lapointe, M., Jahandideh, H., Farner, J. M. & Tufenkji, N. Super-bridging fibrous materials for water treatment. *Npj Clean Water* **5**, 11 (2022).

29. Kurusu, R. S., Lapointe, M. & Tufenkji, N. Sustainable iron-grafted cellulose fibers enable coagulant recycling and improve contaminant removal in water treatment. *Chem. Eng. J.* **430**, 132927 (2022).

30. Armstrong, O., Kaneda, M., Kalogerakis, G., Lapointe, M. & Tufenkji, N. Quaternary ammonium–modified cellulose fibers can enhance wastewater treatment performance under challenging conditions. *Sep. Purif. Technol.* **398**, 138125 (2026).

31. Kaneda, M. *et al.* Effective removal of microplastics and Nanoplastics with cationic cellulose fibers in wastewater treatment. *Chem. Eng. J. Green Sustain.* 100097 (2026) doi:10.1016/j.cejgas.2026.100097.

32. Mebarki, M., Joge Ngale, G. & Lapointe, M. Fibrous super-bridging agents simultaneously improve contaminants removal and sludge dewatering via a very compact three-in-one process. *Npj Clean Water* **8**, 11 (2025).

33. Hube, S. & Wu, B. Mitigation of emerging pollutants and pathogens in decentralized wastewater treatment processes: A review. *Sci. Total Environ.* **779**, 146545 (2021).

34. Canadian Council of Ministers of the Environment. *Canadian Water Quality Guidelines for the Protection of Aquatic Life: Total Particulate Matter*. 13 (2002).

35. United States Environmental Protection Agency. *Developing Water Quality Criteria for Suspended and Bedded Sediments (SABs) - Potential Approaches*. 59 (2003).

36. Sridang, P., Thongmak, N., Danteravanich, S. & Grasmick, A. Stability of skim latex suspension and rubber content recovery by microfiltration process: operating conditions and fouling characteristics. *Desalination Water Treat.* **45**, 70–78 (2012).

37. MELCC. Règlement sur les ouvrages municipaux d’assainissement des eaux usées chapitre Q-2. R. 34.1. (2013).

38. Alioua, W. & Lapointe, M. Fiber-based super-bridging agents enable efficient contaminant removal via settling and screening: Impact on microplastics, textile fibers, and turbidity. *J. Environ. Chem. Eng.* **11**, 110195 (2023).

39. Blancho, F., Lapointe, M., Quevedo, A. C., Kannan, K. & Tufenkji, N. Demonstrating scale-up of a novel water treatment process using super-bridging agents. *Water Res.* **254**, 121301 (2024).

40. Slavov, A. K. General Characteristics and Treatment Possibilities of Dairy Wastewater – A Review. *Food Technol. Biotechnol.* **55**, 14–28 (2017).

41. Kaur, N. Different treatment techniques of dairy wastewater. *Groundw. Sustain. Dev.* **14**, 100640 (2021).

42. Ramsuroop, J., Gutu, L., Ayinde, W. B., Basitere, M. & Manono, M. S. A Review of Biological Processes for Dairy Wastewater Treatment and the Effect of Physical Parameters Which Affect Their Efficiency. *Water* **16**, 537 (2024).

43. Kurusu, R. S., Lapointe, M. & Tufenkji, N. Sustainable iron-grafted cellulose fibers enable coagulant recycling and improve contaminant removal in water treatment. *Chem. Eng. J.* **430**, 132927 (2022).

44. Raissouni, B., Benkara, L. M. & Lapointe, M. Fiber-based super-bridging agents improve flotation and settling during water treatment. *J. Water Process Eng.* **63**, 105499 (2024).

45. Rahman, N. S. A., Yhaya, M. F., Azahari, B. & Ismail, W. R. Utilisation of natural cellulose fibres in wastewater treatment. *Cellulose* **25**, 4887–4903 (2018).

46. Bolto, B. & Gregory, J. Organic polyelectrolytes in water treatment. *Water Res.* **41**, 2301–2324 (2007).

47. Ministère de l'Environnement et de la Lutte contre les changements climatiques (MELCC). Guide pour l'établissement des normes de rejet d'une installation de traitement des eaux usées d'origine domestique. (2020).

48. Hernández-Chover, V., Castellet-Viciano, L., Fuentes, R. & Hernández-Sancho, F. Circular economy and efficiency to ensure the sustainability in the wastewater treatment plants. *J. Clean. Prod.* **384**, 135563 (2023).

49. Cairone, S. *et al.* Revolutionizing wastewater treatment toward circular economy and carbon neutrality goals: Pioneering sustainable and efficient solutions for automation and advanced process control with smart and cutting-edge technologies. *J. Water Process Eng.* **63**, 105486 (2024).

50. Brooks, B. W. *et al.* Identifying Priority Research Questions for Decentralized Wastewater. *Environ. Sci. Technol.* **60**, 49–63 (2025).

51. Kim, J.-W., Lim, H.-B. & Shin, H.-S. Toward enhancing the reliability of particulate organic carbon analysis in aquatic systems: A new perspective on particle settling and pretreatment improvement. *Microchem. J.* **218**, 115602 (2025).

52. Lapointe, M., Kurusu, R. S., Hernandez, L. M. & Tufenkji, N. Removal of Classical and Emerging Contaminants in Water Treatment Using Super-Bridging Fiber-Based Materials. *ACS EST Water* **3**, 377–386 (2023).

53. Mebarki, M. & Lapointe, M. Impact of iron-(hydr)oxide functionalized cellulose fibers on petrochemical wastewater treatment. *ChemRxiv* **2025**,.

54. Kaneda, M. *et al.* Effective Removal of Microplastics and Nanoplastics with Cationic Cellulose Fibers in Wastewater Treatment. *ChemRxiv* **2026**,.

55. Yang, H. & van de Ven, T. G. M. Preparation of hairy cationic nanocrystalline cellulose. *Cellulose* **23**, 1791–1801 (2016).

56. Lapointe, M. & Barbeau, B. Dual starch–polyacrylamide polymer system for improved flocculation. *Water Res.* **124**, 202–209 (2017).

57. Lapointe, M. & Barbeau, B. Selection of media for the design of ballasted flocculation processes. *Water Res.* **147**, 25–32 (2018).